Original article

Enhanced critical-sized bone defect repair efficiency by combining deproteinized antler cancellous bone and autologous BMSCs

Jin-Qi Wei[a,b,1], Yun Liu[a,c,1], Xue-Hui Zhang[d,e,f,**], Wei-Wei Liang[a], Tuan-Feng Zhou[b], Hua Zhang[b], Xu-Liang Deng[a,e,f,*]

[a] Department of Geriatric Dentistry, Peking University School and Hospital of Stomatology, Beijing 100081, China
[b] First Clinical Division, Peking University School and Hospital of Stomatology, Beijing 100034, China
[c] Department of Prosthodonitcs, Peking University School and Hospital of Stomatology, Beijing 10081, China
[d] Department of Dental Materials & Dental Medical Devices Testing Center, Peking University School and Hospital of Stomatology, Beijing 100081, China
[e] National Engineering Laboratory for Digital and Material Technology of Stomatology, Peking University School and Hospital of Stomatology, Beijing 100081, China
[f] Beijing Laboratory of Biomedical Materials, Peking University School and Hospital of Stomatology, Beijing 100081, China

A B S T R A C T

Previously we have demonstrated that calcinated antler cancellous bone (CACB) has great potential for bone defect repair, due to its highly similar composition and architecture to natural extracellular bone matrix. This study is aiming at seeking for an optimal strategy of combined application of CACB and bone marrow mesenchymal stem cells (BMSCs) in bone defect repair. In vitro study demonstrated that CACB promoted the adhesion, spreading and viability of BMSCs. Increased extracellular matrix production and expression of osteogenic markers in BMSCs were observed when seeded on CACB scaffolds. The cells ceased to proliferation in the dual effect of CACB and osteogenic induction at the early stage of incubation. Hence synergistic effect of CACB combined with autologous undifferentiated BMSCs in rabbit mandible critical-sized defect repair was further evaluated. Histological analysis results showed that loading the CACB with autologous BMSCs resulted in enhanced new bone formation and angiogenesis when compared with implanted CACB alone. These findings indicate that the combination of CACB and autologous BMSCs should become potential routes to improve bone repair efficiency

© 2017 Chinese Chemical Society and Institute of Materia Medica, Chinese Academy of Medical Sciences. Published by Elsevier B.V. All rights reserved.

1. Introduction

In oral and maxillofacial surgery, and orthopedic surgery, large bone defects repair with desired results is still a substantial clinical challenge. Xenogenic bone grafts are widely used in repair of bone defect in clinic for their excellent osteoconductivity, biosecurity and accessibly [1]. However, the clinical outcome is not always satisfactory due to the lack of functional cells and bioactive growth factors. The technology of bone tissue engineering brings light on better application of xenogenic bone grafts. The fundamental concept of tissue engineering is to utilize seed cells and/or grow factors to endow the scaffolds properties of osteoinductivity and osteogenesis. This strategy has gained a lot of success. Kon E et al. reported that loading autologous bone marrow mesenchymal stromal cells onto porous hydroxyapatite ceramic resulted in better bone repair efficacy compared with cell-free implants in the critical-size defects of sheep long bones [2]. The study of Bareille, R. et al. demonstrated that implanted subcutaneously an osteoconductive hydroxyapatite matrix (ENDOBON) loaded with human bone marrow cells (HBMSC) in athymic mice giving rise to an early lamellar bone formation only in the pores of hydroxyapatite loaded with HBMSC [3]. Similar results have been obtained with Bio-Oss® combined with BMSCs in sinus augmentations in adult sheep [4]. In previous studies, we developed a new source of inorganic xenogenic bone substitute-deproteinized antler cancellous bone (CACB), which has the advantages of good reproducibility and easy accessibility and is acceptable in terms of animal welfare and ethical considerations [5]. With highly similar mineral

---

composition, physical properties, and interconnecting pore structures to human cancellous bone, CACB has potential for utilization in bone defect repairs [5]. However, the efficacy of bone defect repair using CACB only is not satisfactory due to the lack of functional cells and bioactive growth factors. To solve this issue, our further studies had shown that the bone defect repair efficacy of CACB could be improved by combining bioactive molecules [6] or adipose-derived stem cells (ADSCs) [7].

In the field of bone tissue engineering, adipose and bone marrow are most common source of mesenchymal stem cells. ADSCs can be obtained in large quantities under local anesthesia by liposuction is a rich source of mesenchymal stem cells [8]. However, the lower ability of osteogenic differentiation and the possibility of changing into fat tissue for ADSCs limit their wide application in clinic. Alternatively, bone marrow-derived stromal cells (BMSCs) with high osteogenic differentiation ability become the promising seed cells and gain extensively acceptance in bone defect repair for their efficacy and safety [9–11]. Concerning the further effective clinical application, the therapeutic efficacy of combination of BMSCs and CACB in bone defect repair should be clarified.

Hence, the purpose of this study is to evaluate the effects of CACB on the behaviors of BMSCs *in vitro* and the efficiency of CACB in improving bone defect repair by combining autologous BMSCs *in vivo*. The physicochemical properties of CACB were firstly investigated, including the microstructure and apatite morphology. The effect of CACB scaffolds on the bioactivity of isolated rabbit BMSCs, in terms of attachment, proliferation and osteogenic differentiation *in vitro* was then evaluated. Finally, the efficacy of the CACB in combination with autologous BMSCs in rabbit mandible defect repair was explored to confirm their clinical potential.

2. Results and discussion

2.1. Characterization of CACB scaffolds

CACB was white and porous scaffold in gross view (Fig. 1A). To capture more details about CACB, we used scanning electric microscopy (SEM). Well-interconnected macro-pores range about 300–700 μm in size were shown in SEM images (Fig. 1B). The basic elements of the CACB were hydroxyapatite (HA) crystals that are 400–600 nm in width and 5–15 mm in length (Fig. 1C). Previous studies showed that pore sizes >300 mm and porosity ranging from 70% to 80% are optimal for enhanced vascularization and osteogenesis, due to appropriate exchange and supply of oxygen and nutrients [12,13]; the microstructure of CACB had been proved to be benefit for mesenchymal stromal cells such as ADSCs spreading and osteogenic differentiation [7]. Thus, the structure of CACB could favor the activity of BMSCs *in vitro* and bone regeneration *in vivo*.

2.2. Cell adhesion and proliferation of BMSCs on CACB

To observe the cell adhesion and proliferation of BMSCs on CACB scaffolds. The cells morphology was captured with SEM and Confocal Laser Scanning Microscopy (CLSM) at day 1, 3 and 7 after seeding. At the 1 st day after seeding, BMSCs show highly branched morphology with pseudopodia spreading on the surface of CACB (Fig. 2A). After 7 days of cultivation, large amount of BMSCs cover the trabeculae and span over the pores (Fig. 2B). The growth activity of BMSCs on CACB scaffolds was improved with prolonged incubation time. Quantized evaluation of the proliferation was
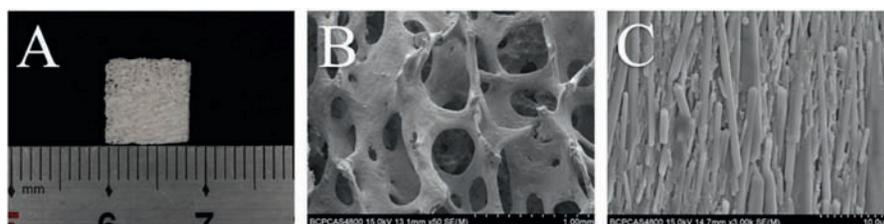

Fig. 1. Morphology and structure of CACB. (A) Macroscopic image; (B) SEM image of porous structure of CACB; (C) SEM image of CACB crystals morphology at high magnification.
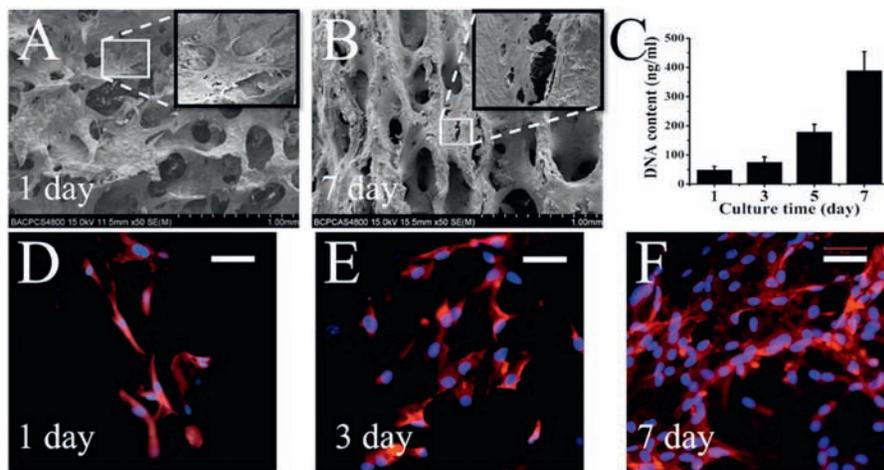

Fig. 2. The bioactivity of BMSCs on CACB scaffolds. (A, B) SEM images of BMSCs adhesion and morphologies on CACB scaffolds after 1 and 7 days of incubation. (C) DNA content of BMSCs seeded on CACB. (D, E, F) CLSM images of BMSCs on CACB observed. (Scale bar = 50 μm).
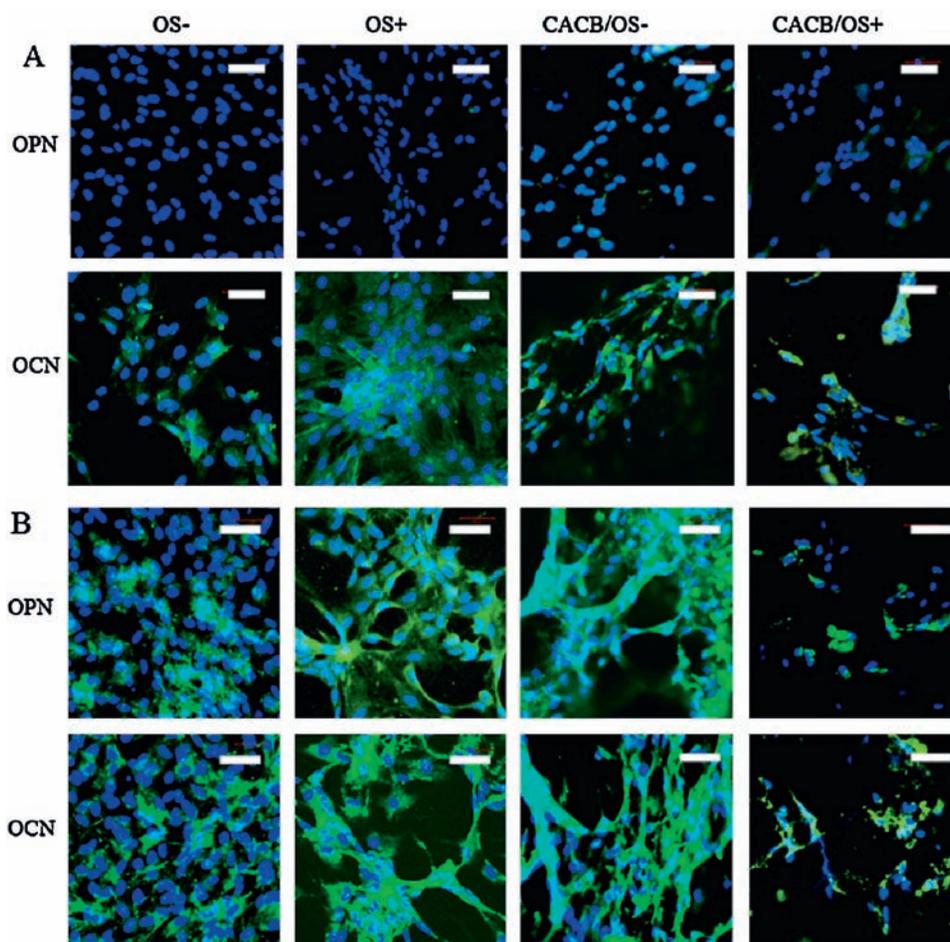
Fig. 3. Immunofluorescence staining of osteopontin (OPN) and osteocalcin (OCN) in BMSCs cultured for 7 (A) and 14 days (B). (Scale bar = 50 μm).

taken out with monitoring the change of DNA content in cells growing in CACB. Result suggested the cells enter the logarithmic growth phase on the 3rd day (Fig. 2C). These were consistent with the observation of CLSM at 1, 3 and 7 days after seeding (Fig. 2D-F). These results demonstrated that the microenvironment constructed by multi-scale topography and biomimetic chemical component of CACB scaffolds improved BMSCs viability and promoted the cells to extend dense pseudopodia to form a highly branched morphology. Such biocompatibility between scaffolds and cells is important for the bone defect healing process. Muller *et al.* and Cui *et al.* reported that a natural architecture of bovine-derived xenogenic bone grafts benefit mesenchymal stem cell adhesion and improve their proliferation [14,15]. Besides the physical structure of CACB, the chemical components including trace amounts of Si and Zn ions found in our previous study[16] can also improve bioactivity of BMSCs as described in others researches [17–22].

2.3. Osteogenic differentiation of BMSCs on CACB scaffolds

The outcome of bone defect repair after implanted xenografts into target area is largely determined by how the microenvironments formed by the physiochemical properties of xenografts affect the bioactivity and differentiation of the seed cells [23,24]. Hence, it is necessary to elucidate the process of the osteogenic differentiation of BMSCs on CACB.

In this study, secreted osteogenic marker protein OPN and OCN, temporal kinetics of the mRNA expression of ALP, BMP2, OPN, OCN, BSP and RUNX2 in BMSCs, detected by immunofluorescence

staining and Real-time quantitative polymerase chain reaction (RT-qPCR) separately, were used to evaluate the osteogenic behavior of BMSCs on CACB scaffolds. As shown in Fig. 3, the CACB could drive BMSCs down the osteogenic lineage without using osteogenic supplements, which was consistent with our previous study [7]. At 7th day, no matter OS induction presence or not, CACB promoted the secretion of OCN in the BMSCs. Similar staining intensities were detected in both the CACB/OS- group and OS+ group. No visible OPN presence in any group. After 14 days, significantly increased production of OPN and OCN were detected in all the groups compared with those on day 7. On day 14, both the CACB/OS- and OS+ groups showed similar intensities. Further more, higher expression level of osteogenic marker gene mRNA in BMSCs seeded in CACB than that in negative control but lower than that in positive control at early stage (the 7th day), and almost the same between CACB group and positive control at later stage (the 14th day), detected by RT-qPCR (Fig. 4). The results suggested that CACB alone possesses the capability of driving BMSCs down the osteogenic lineage, though not as strong as the effect of osteogenic induction medium. Despite the controversial opinions regarding whether the xenogenic grafts possess the capability of promoting osteogenic differentiation [15,25–27], these results once again demonstrated the capability of CACB in osteogenic differentiation.

An interesting phenomenon found in this study was that the number of cells in CACB/OS+ group kept almost the same on both the 7th day and 14th day and significantly less than that in CACB/OS- group as shown in immunofluorescence staining results (Fig. 3). This suggested that the synergistic effect of CACB and osteogenic induction might be too strong to turn BMSCs into
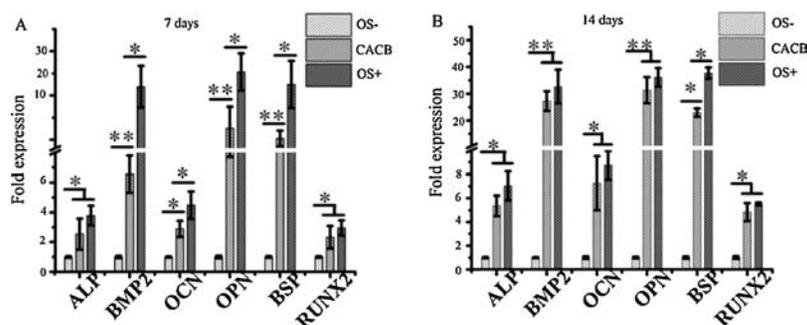
Fig. 4. Gene expression profiles of ALP, BMP2, OPN, OCN, BSP and RUNX2 analyzed by RT-qPCR after 7 (A) and 14 days (B) of cultivation. Cells cultured in common medium (OS−) were used as the control group. *$P < 0.05$ and ** $P < 0.01$.
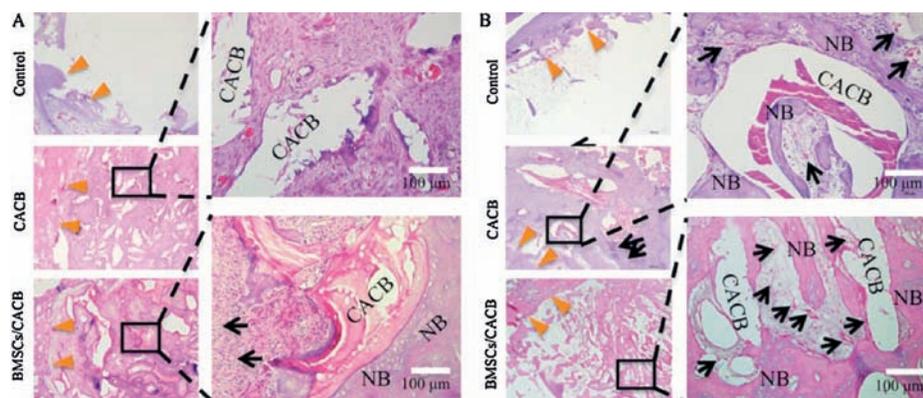

Fig. 5. Bone defect repair in rabbit mandibles defect models after implantation of auto-BMSCs/CACB. (A) Histological analysis of new bone formation by hematoxylin and eosin (H&E) staining at 4 weeks. (B) Histological analysis of new bone formation and growth of blood vessels by H&E staining at 12 weeks. (NB, nascent bone, BV, blood vessels; Orange arrow denote boundary of bone defects; Black arrows denote new blood vessels).

osteoblasts in the early stage of incubation and made them cease to proliferation.

2.4. Efficacy of auto-BMSCs/CACB composites in improving bone defects repair

The *in vivo* osteogenic capacity of the autologous BMSCs/CACB composites in critical-sized bone defect repair was further investigated. Base on the *in vitro* results, to obtain more functional cells for *in vivo* study, BMSCs were cultured with common medium for 7 days after seeded on CACB scaffolds before implanted into critical-sized defects of rabbit mandible.

The histological evaluation revealed that loading of BMSCs into CACB increased the quality and quantity of new bone formation, as shown in Fig. 5. At 4 weeks post-implantation, unhealed defect filling with fat tissue were observed in the control group. A small amount of new bone leaning on the scaffolds was found in the CACB group, while much more new bone appeared in the BMSCs/ CACB group. At 12 weeks post implantation, there was still little new bone observed in the control group. The auto-BMSCs/CACB implantation resulted in the formation of mature and regular bony trabeculae, while fewer and immature trabeculae were found in the CACB group. These could be ascribed to factors including the nano-/micro-sized topography, released Ca, P, Zn and Si ions from CACB, which are benefit for keeping the viability of BMSCs and promoting them down an osteogenic linage.

More interestingly, significantly improved vascularization after implantation of auto-BMSCs/CACB composites was observed compared to CACB implantation only (Fig. 5B). Firstly, this could be ascribed to the presence of iron (Fe) element in CACB found in our previous study [16], which has been shown to increase osteogenesis and neovascularization [28]. More importantly, the cell-cell interaction effect between endothelial cells and BMSCs endowed auto-BMSCs/CACB composites with the outstanding neovascularization. BMSCs can secrete vascular endothelial growth factor, fibroblast growth factor and hematopoietic growth factor, which are of vital importance to the migration and proliferation of endothelial cells. Meanwhile, the ingrown blood vessels can not only transport oxygen and nutrition, but also secrete BMP2, which could, in turn, promote osteogenesis [29].

3. Conclusion

In this study, the biologic behaviors including attachment, proliferation and osteogenic differentiation of BMSCs in CACB were investigated. The biomimetic multi-scale topography and chemical niches provided by CACB could not only promote BMSCs viability and favor cell attachment and spreading, but also drive them down an osteogenic lineage without osteogenic induction. Based on the *in vitro* study, synergistic effects of autologous BMSCs and CACB in improving critical-sized rabbit mandible defect were evaluated. The improved bone repair efficiency was observed in the implantation of auto-BMSCs/CACB composites. These findings may promote the clinic application of CACB and the reasonable use of seed cells/bio-scaffolds combination in bone tissue engineering.

4. Experimental

4.1. Preparation and Characterization of CACB scaffolds

The CACB scaffolds were prepared as our previous report [5]. The surface morphology and structure were observed using scanning electron microscopy (SEM; ZEISS, Supra 55) after the samples were sputter coated with gold at a voltage of 15.0 kV.

Table 1
Primers used in RT-qPCR.

Gene		Sequence (5′-3′)	No.
ALP	Forward	TCAGCTTCCTCCTCTTTGCG	XM_002716044.1
	Reverse	CGGGTCCACAGTTCAGGAAA	
BMP2	Forward	ACTGCCAGAAACAAGTGGGA	NM_001082650.1
	Reverse	TGATGGAAACCGCTGTCGTC	
OPN	Forward	TGGCTAAACCCTGACCCAT	NM_001082194.1
	Reverse	TATCCACGTGGTCATCGTCC	
OCN	Forward	AGAGTCTGGCAGAGGCTCA	XM_002715383.3
	Reverse	CAGGGGATCCGGGTAAGGA	
BSP	Forward	ACGCTTTCTTTCACAACACCTG	XM_002717020.1
	Reverse	GCTGGTGCCATTGATGCTCTG	
RUNX2	Forward	TCTGGCCTTCCACTCTCAGTA GGCGGGGTGTAAGTAAAGGT	XM_008262992
	Reverse		
GAPDH	Forward	GTATGATTCCACCCACGGCA	NM_001082253.1
	Reverse	CCAGCATCACCCCACTTGAT	

4.2. Isolation and culture of rabbit BMSCs

Twelve male New Zealand White rabbits weighing about 1.5 kg (Center of Experimental Animal, Peking University School and Hospital of Stomatology) were used. The experimental protocol was approved by the Animal Care and Use Committee of Peking University. Bone marrow was extracted from the iliac bone of the 12 rabbits for *in vitro* culture of the BMSCs. The cells were cultured with common medium (10% fetal bovine serum in Dulbecco's modified Eagle's medium, containing 1% penicillin/streptomycin; Cyagen Biosciences, Inc.) and typically passaged when 80% confluent.

4.3. Cell morphology observation on CACB scaffold

About 4×10^5 BMSCs at a density of 2×10^6 cells/mL were seeded on each scaffold in a 6-well plate (Corning, Inc.), and cultured with the common medium. After 1 and 7 days, the cells were fixed with 2.5% glutaraldehyde, afterward immersed in a 0.18 mol/L saccharose solution for 2 h, and then dehydrated using an increasing ethanol gradient. The samples were dried overnight, sputter-coated with gold, and observed using SEM at 15 kV.

4.4. Cell proliferation analysis

After being cultured for 1, 3, and 7 days, discarded the supernatant and the cells were fixed with 4% paraformaldehyde. The F-actin filaments were stained with 50 mg/ml rhodamine phalloidin (Sigma-Aldrich). The nuclei were stained using 0.3 mmol/L 4′, 6′-diamidoino-2-phenylindole (DAPI; Sigma-Aldrich). Confocal laser scanning microscopy (CLSM; Carl Zeiss) was used to qualitatively monitor cell proliferation on CACB.

A quantitative analysis of cell proliferation by monitoring the cell DNA content using Quant-iTTM dsDNA HS Assay Kit (Invitrogen) was also performed. Triple separate experiments were repeated.

4.5. Immunofluorescence staining of OPN and OCN

The cells were cultured in 4 different culture conditions in this experiment: the CACB/OS- group, BMSCs seeded in CACB and cultured in common medium; the CACB/OS+ group, BMSCs seeded in CACB and cultured in osteoinductive medium (OS, common medium containing 10 nmol/L dexamethasone, 20 mmol/L β-glycerophosphate, 0.05 mmol/L ascorbic acid); the OS- group, cells cultured with common medium; and the OS+ group, cells cultured with osteoinductive medium. At 7th and 14th day, after fixed with 4% paraformaldehyde, the cells were permeabilized with 0.1% Triton X-100/phosphate-buffered saline for 5 min, blocked with 3%

bovine serum albumin, and then incubated with a 1:500 dilution of the primary antibodies to osteopontin (OPN; custom made from Abcam, Inc.) or osteocalcin (OCN; Abcam, Inc.) overnight at 4 °C. Afterward, the cells were incubated with a 1:250 dilution of the secondary antibody (FITC-conjugated Affinipure goat anti-mouse IgG; Abcam, Inc.). Finally, cell nuclei were stained with DAPI. The staining intensities of OCN, and OPN were observed using CLSM.

4.6. Real-time quantitative PCR analysis

Three groups were included in this experiment: The CACB group, BMSCs seeded in CACB and cultured in common medium; the OS- group, cells cultured with common medium; and the OS+ group, cells cultured with osteoinductive medium. At 7th and 14th day, cells were lysed with Trizol Reagent (Ambion) and total RNA was extracted. The ReverTra Ace qPCR RT Master Mix (Toyobo Co., Ltd.) was used to synthesize first-strand cDNA. Real-time quantitative polymerase chain reaction (RT-qPCR) using Fast-Start Universal SYBY Green Master (Rox; Roche Ltd.) was performed with a 7500 Real-Time PCR System (Life Technologies, Inc.). Relative quantification was carried out using the $2^{-\Delta\Delta Ct}$ method. Three separate experiments were performed. The primer sequences of osteogenic genes including alkaline phosphatase (ALP), bone Morphogenetic Protein 2 (BMP2), OPN, OCN, bone sialoprotein (BSP) and runt-related transcription factor 2 (RUNX2) are listed in Table 1.

4.7. In vivo osteogenesis of CACB combined with BMSCs

Preparation of auto-BMSCs/CACB composites: About 1.5×10^6 auto-BMSCs from each rabbit were seeded on 0.25 mg CACB with size about 1.0–2.0 mm in diameter, and then cultured in common medium for 7 days. And BMSCs/CACB composites were prepared for *in vivo* study.

Surgical procedures: The critical sized bone defects (8 mm in diameter) in each side of the mandibles of 12 rabbits were created as described in our previous report [5] and were randomly divided into three groups: (1) CACB group: eight defects implanted with 0.25 mg CACB granules; (2) BMSCs/CACB group: eight defects implanted with auto-BMSCs/CACB composites; and (3) Control group: eight defects were left untreated. Rabbits were sacrificed using lethal intravenous administrations of sodium pentobarbital at 4 and 12 weeks post implantation.

References

[1] H.F. Nasr, M.E. Aichelmann-Reidy, R.A. Yukna, Bone and bone substitutes, Periodontology 19 (1999) (2000) 74–86.

[2] E. Kon, A. Muraglia, A. Corsi, et al., Autologous bone marrow stromal cells loaded onto porous hydroxyapatite ceramic accelerate bone repair in critical-size defects of sheep long bones, J. Biomed. Mater. Res. 49 (2000) 328–337.

[3] R. Bareille, M.H. Lafage-Proust, C. Faucheux, et al., Various evaluation techniques of newly formed bone in porous hydroxyapatite loaded with human bone marrow cells implanted in an extra-osseous site, Biomaterials 21 (2000) 1345–1352.

[4] R. Gutwald, J. Haberstroh, J. Kuschnierz, et al., Mesenchymal stem cells and inorganic bovine bone mineral in sinus augmentation: comparison with augmentation by autologous bone in adult sheep, Br. J. Oral. Maxillofac. Surg. 48 (2010) 285–290.

[5] X. Zhang, Q. Cai, H. Liu, et al., Osteoconductive effectiveness of bone graft derived from antler cancellous bone: an experimental study in the rabbit mandible defect model, Int. J. Oral. Maxillofac. Surg. 41 (2012) 1330–1337.

[6] X.H. Zhang, M.M. Xu, L. Song, et al., Effects of compatibility of deproteinized antler cancellous bone with various bioactive factors on their osteogenic potential, Biomaterials 34 (2013) 9103–9114.

[7] J.Q. Wei, M.M. Xu, X.H. Zhang, et al., Enhanced osteogenic behavior of ADSCs produced by deproteinized antler cancellous bone and evidence for involvement of ERK signaling pathway, Tissue Eng. Part A 21 (2015) 1810–1821.

[8] H. Mizuno, Adipose-derived stem cells for tissue repair and regeneration: ten years of research and a literature review, J. Nippon Med. Sch. 76 (2009) 56–66.

[9] Y. Yamada, S. Nakamura, K. Ito, et al., Injectable tissue-engineered bone using autogenous bone marrow-derived stromal cells for maxillary sinus augmentation: clinical application report from a 2-6-year follow-up, Tissue Eng. A 14 (2008) 1699–1707.

[10] D. Dallari, L. Savarino, C. Stagni, et al., Enhanced tibial osteotomy healing with use of bone grafts supplemented with platelet gel or platelet gel and bone marrow stromal cells, J. Bone Jt. Surg. Am. 89 (2007) 2413–2420.

[11] Z. Gamie, G.T. Tran, G. Vyzas, et al., Stem cells combined with bone graft substitutes in skeletal tissue engineering, Expert Opin. Biol. Ther. 12 (2012) 713–729.

[12] V. Karageorgiou, D. Kaplan, Porosity of 3D biomaterial scaffolds and osteogenesis, Biomaterials 26 (2005) 5474–5491.

[13] P. Kasten, I. Beyen, P. Niemeyer, et al., Porosity and pore size of β-tricalcium phosphate scaffold can influence protein production and osteogenic differentiation of human mesenchymal stem cells: an in vitro and in vivo study, Acta Biomater. 4 (2008) 1904–1915.

[14] P. Müller, U. Bulnheim, A. Bulnheim, et al., Calcium phosphate surfaces promote osteogenic differentiation of mesenchymal stem cells, J. Cell. Mol. Med. 12 (2008) 281–291.

[15] L. Cui, B. Liu, G.P. Liu, et al., Repair of cranial bone defects with adipose derived stem cells and coral scaffold in a canine model, Biomaterials 28 (2007) 5477–5486.

[16] S. Meng, X.H. Zhang, M.M. Xu, et al., Effects of deer age on the physicochemical properties of deproteinized antler cancellous bone: an approach to optimize osteoconductivity of bone graft, Biomed. Mater. 10 (2015) 035006.

[17] H.L. Sun, C.T. Wu, K.R. Dai, J. Chang, T.T. Tang, Proliferation and osteoblastic differentiation of human bone marrow-derived stromal cells on akermanite-bioactive ceramics, Biomaterials 27 (2006) 5651–5657.

[18] M. Amaral, M.A. Costa, M.A. Lopes, et al., Si_3N_4-bioglass composites stimulate the proliferation of MG63 osteoblast-like cells and support the osteogenic differentiation of human bone marrow cells, Biomaterials 23 (2002) 4897–4906.

[19] M.B. Nair, A. Bernhardt, A. Lode, et al., A bioactive triphasic ceramic-coated hydroxyapatite promotes proliferation and osteogenic differentiation of human bone marrow stromal cells, J. Biomed. Mater. Res. A 90 (2009) 533–542.

[20] M. Honda, K. Kikushima, Y. Kawanobe, et al., Enhanced early osteogenic differentiation by silicon-substituted hydroxyapatite ceramics fabricated via ultrasonic spray pyrolysis route, J. Mater. Sci. Mater. Med. 23 (2012) 2923–2932.

[21] X.M. Luo, D. Barbieri, N. Davison, et al., Zinc in calcium phosphate mediates bone induction: in vitro and in vivo model, Acta Biomater. 10 (2014) 477–485.

[22] S.A. Oh, S.H. Kim, J.E. Won, et al., Effects on growth and osteogenic differentiation of mesenchymal stem cells by the zinc-added sol-gel bioactive glass granules, J. Tissue Eng. 2010 (2011) 475260.

[23] J.I. Dawson, R.O.C. Oreffo, Bridging the regeneration gap: stem cells, biomaterials and clinical translation in bone tissue engineering, Arch. Biochem. Biophys. 473 (2008) 124–131.

[24] Z.F. Lu, S.I. Roohani-Esfahani, G.C. Wang, H. Zreiqat, Bone biomimetic microenvironment induces osteogenic differentiation of adipose tissue-derived mesenchymal stem cells, Nanomed. Nanotechnol. Biol. Med. 8 (2012) 507–515.

[25] Y. Açil, H. Terheyden, A. Dunsche, B. Fleiner, S. Jepsen, Three-dimensional cultivation of human osteoblast-like cells on highly porous natural bone mineral, J. Biomed. Mater. Res. 51 (2000) 703–710.

[26] A. Kubler, J. Neugebauer, J.H. Oh, M. Scheer, J.E. Zöller, Growth and proliferation of human osteoblasts on different bone graft substitutes: an in vitro study, Implant. Dent. 13 (2004) 171–179.

[27] K. Siggers, H. Frei, G. Fernlund, F. Rossi, Effect of bone graft substitute on marrow stromal cell proliferation and differentiation, J. Biomed. Mater. Res. A 94 (2010) 877–885.

[28] V.S. Chandra, G. Baskar, R.V. Suganthi, et al., Blood compatibility of iron-doped nanosize hydroxyapatite and its drug release, ACS Appl. Mater. Interfaces 4 (2012) 1200–1210.

[29] H.Y. Li, K. Xue, N. Kong, K. Liu, J. Chang, Silicate bioceramics enhanced vascularization and osteogenesis through stimulating interactions between endothelia cells and bone marrow stromal cells, Biomaterials 35 (2014) 3803–3818.